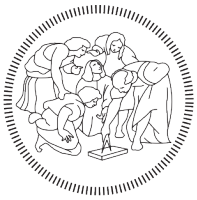

POLITECNICO
MILANO 1863

Analysis of bipropellant liquid engine for CubeSats

Bovisa Rocketry Industries
Giulio Corsi - 944379
Grusovin Sofia - 940015
Kannabiran Lokeswari – 927001
Lardo Gianluca - 945857
Mascetti Stefano - 940314
Murugan Shanmuga Priya – 926978
Murer Riccardo Giovanni - 844606
Stratan Vasile - 873957

Final Report

Course of Space Propulsion
School of Industrial Engineering
Academic Year 2019-2020

Contents

List of Figures

List of Tables

Chapter 1

Introduction

The term CubeSat is used to describe a small satellite whose basic unit form is a 10 *cm* edge cube, namely 1U. CubeSat units can be put together to form bigger artifacts, like 2U, 3U, 6U, and so forth. When the first CubeSats were launched in the early 2000s, there was a general perception that they were just toy satellites designed to fulfil the needs of student training or to meet some amateur demands. Later, it was understood that CubeSats could also be used for other applications, such as testing of technologies and science missions, like those related to astronomy and space weather.

1.1 Motivation

CubeSats are miniature satellites that provide a cost-effective means to perform a scientific and technical study in space. They have been used for interplanetary missions for more than a decade. Due to their small sizes, CubeSats are only treated as a secondary payload. CubeSats have mainly been restricted in their operations due to their small sizes that limit their on-board capabilities leading to limited mission life and range of travel. This workshop aims to design a mini bipropellant system for CubeSats for a long term space mission and to study their important performance factors. What makes the bipropellant engines more advantageous than other chemical devices such as mono-propellant thrusters, is the higher specific impulse that leads to savings in propellant mass. What makes the system disadvantageous, is the complexity. Since the component part count is high, it increases the dry mass thus making it feasible only for high Δv requiring missions.

1.2 Literature survey

The use of bipropellant engines with low thrust ranges has been under study in the last decade. Several propulsion solution manufacturers have developed devices working in the $< 22\,N$ range. Up to now, these engines are seen as a new propulsion device for attitude control system of larger spacecrafts. The coupling with the primary propulsion eliminates the need of separate propellant and pressurizer tanks.

The authors of [1] provide an overview of micro-propulsion technologies that have been developed or are currently being developed for CubeSats. The paper [2] provides a throughout discussion on the different propulsion technologies used for CubeSat and other micro-satellite systems.

Aerojet Liquid Rocket Company proved the feasibility of a 22 N thrust engine based on N_2O_4/MMH propellant [3]. They managed to obtain a 8 hours steady-state firing with a minimum impulse bit $< 0.022\,N$, and specific impulse of 275 s. Moreover, valve response, repeatability, life, engine minimum impulse bit, together with all aspects of engine fabrication techniques have been demonstrated.

Developing an engine for Kinetic Energy Anti Satellite [4], Rockwell managed to eliminate the need of film cooling (accounting 30-40% of the fuel) by using high temperature materials for the combustion chamber. This resulted in improved combustion and decreased injector head complexity.

In the paper [5], a 30 kg 16U Interplanetary CubeSat mission on a hybrid high-thrust and low-thrust trajectory utilising a Dual Chemical-Electric Propulsion System to achieve Earth escape (high-thrust) and perform autonomous deep-space cruise (low-thrust) to Mars has been described. The design consists of an ADN-based monopropellant thruster and an Ethanol-H_2O_2 based bipropellant thruster and yields to a thrust of 2.91 N and an $I_s = 303.15\ s$, with a weight of 4.85 kg while occupying 6.5U space.

Another successful and green bipropellant engine by Hyperion technologies [6] demonstrated the capability to provide a specific impulse of 285 s and 0.5 N thrust.

Chapter 2

Concept description

2.1 Propellant choice

The mission requires to give a Δv of 600 m/s to the satellite, and the maximum acceleration should not exceed $3g$. The first issue we have to take into account is the choice of the propellant; the satellite has to be designed for a long term mission, so the propellant must be storable for a long period. For this reason, we automatically excluded all the cryogenic propellants. We also discarded gaseous phase propellants due to the volume constraint of the cubesat (such as Methane$_{(g)}$-H_2O_2 couple and N_2O-CH_6 one).

Therefore, our choice laid to use a hypergolic couple to have a more reliable and simpler system. Furthermore, this makes it easier to have multiple engine firings.

Both Hydrazine and MMH have these characteristics, but we chose MMH because of its better performances. In addition to that, the couple MMH-N_2O_4 has been widely used in the space industry history, so its technology is well proven and documented.

The problem with the use of N_2O_4 as an oxidizer is that it freezes at relatively high temperatures (262 K), infact nitric oxide is often added to reduce the freezing point. The obtained mixture of N_2O_4 and NO is called MONi (Mixed Oxides Nitrogen, where "i" is the percentage of nitric oxide). We decided to use MON25 because of its freezing point similar to the one of MMH (218 K). [7]

Table 2.1: Different types of propellant taken into account during the concept phase

	I_s (ε = 100-150)	Ox/Fuel	Density $[kg/m^3]$
Hydrazine N_2O_4	330-340	1.34	Hydrazine: 1000 N_2O_4: 1450
Alcohol H_2O_2	315-321	4.5	Alcohol: 789 H_2O_2: 1450
MMH N_2O_4	330-340	2.16	MMH: 870 N_2O_4: 1450
Kerosene H_2O_2	328-334	7	Kerosene: 800 H_2O_2: 1450

2.2 Architecture

The Figure 2.1 represents the fitting of the propulsion system components inside the frame. Since 4U cubes are rarely adopted due to attitude control-related issues, a standardized platform couldn't be found in the market. Hence, the one that has been used is a representative structure that complies with the standard dimensions of cubesats. Based on [8] the maximum allowed protrusion in the longitudinal direction is of 36 mm length and 64 mm diameter, so it was decided to allow the divergent part of the nozzle to be outside the satellite.

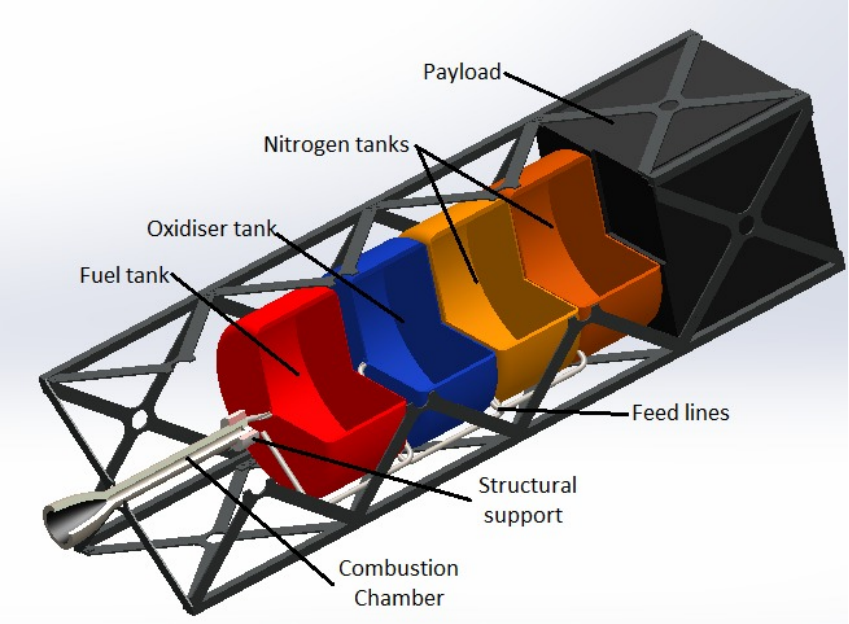

Figure 2.1: General scheme of the propulsion system components inside the structure

The position of the mass center was evaluated at the beginning and at the end of the mission. Due to the selected placement of the tanks, the center of mass will shift along the longitudinal axis of the satellite as presented in Figure 2.2.

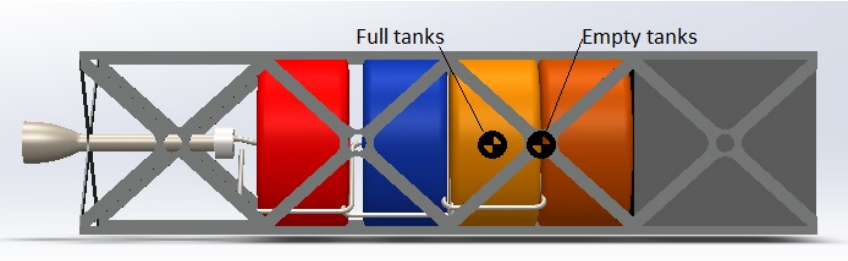

Figure 2.2: Position of the center of gravity and the beginning and at the end of the mission

It is important to design the best pressurization system when it comes to liquid bipropellant engines. Long term missions require storable propellant, hence large volumes for pressurizing gas. To decrease the volume of the gas, a higher pressure is convenient. By implementing the architecture in Figure 2.3 the proper working of the engine is achieved. The cross-feed valve is used to increase the redundancy while valves and pressure regulators are used to control the flow of the fluids during the mission.

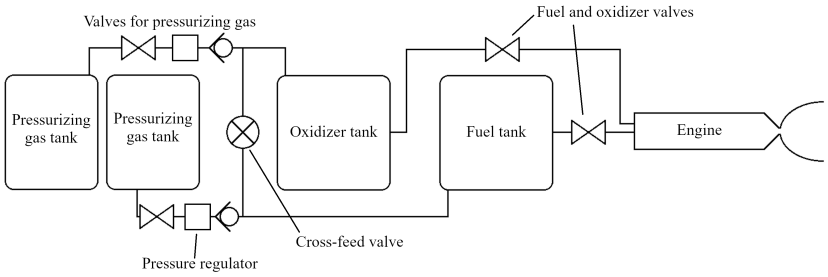

Figure 2.3: Scheme of the pressurization feed system

2.3 CEA Code

To compute the thermodynamic and transport properties of the mixture, we used the CEA program, considering the Bray assumption and setting the freezing point at the throat (simple Bray approach). We set an area ratio of 150, which is a number that guarantees good performances keeping the length of the nozzle to be reasonably short for the Cubesat. The most commonly used combustion chamber pressures for this type of engine are in the range between 6.5 and 15 *bar*. With trial and error, we noted a performance increase proportional with the pressure. However, temperature increases as well, so we decided to set it to 10 *bar*, which was a good trade-off between performances and temperature.

The analysis of the MMH-MON25 couple for different values of oxidizer to fuel ratio reveals a behavior shown in Figure 2.4. Our final choice was to use a slightly fuel rich mixture ratio, in order to have both good performance and limit the combustion chamber temperature. Note: from this point on, we will consider the following assumptions in the computations:

- Monophase gaseous mixture
- Calorically perfect gas

- 1D flow
- Isentropic flow
- Steady adiabatic flow

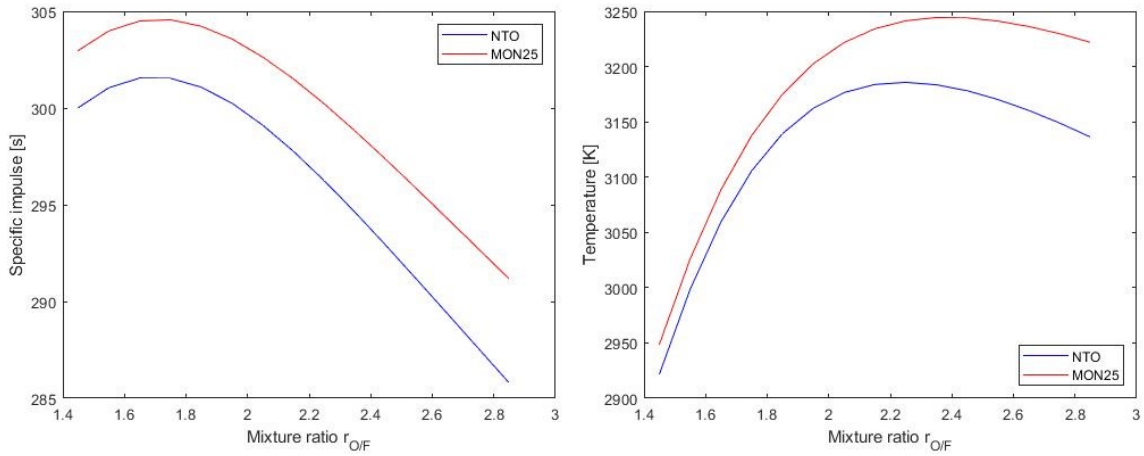

Figure 2.4: Temperature and specific impulse at different mixture ratio values for Nitrogen Tetraoxide and MON25

Table 2.2: Results from CEA Code (ρ, μ and v_{throat} are calculated at throat section)

$r_{O/F}$	ε	P_c $[bar]$	T_c $[K]$	M $[1/n]$	C_p $[KJ/kg\,K]$	ρ $[kg/m^3]$	μ $[mP]$	v_{throat} $[m/s]$
1.55	150	10	3026	19.74	1.586	0.48	0.88	1181

2.4 Performance evaluation

With the thermodynamic properties from the CEA Code it is possible to calculate the characteristic velocity as:

$$c^* = \frac{1}{\Gamma(k)}\sqrt{\frac{\Re}{M}T_c} \qquad \text{, where} \quad \Gamma(k) = \sqrt{k(\frac{2}{k+1})^{\frac{k+1}{k-1}}}$$

To find the exit pressure we used an iterative procedure based on the relation between the pressure and the chosen area ratio, starting from a guess value of 200 Pa. With the external pressure value the thrust coefficient can be found, as well as the specific impulse afterwards:

$$c_T = \sqrt{2(\frac{k^2}{k-1})(\frac{2}{k+1})^{\frac{k+1}{k-1}}}\sqrt{1-(\frac{P_e}{P_c})^{\frac{k-1}{k}}} + \frac{P_e - P_a}{P_c}\varepsilon \quad \text{and} \quad I_s = \frac{c_* c_T}{g_0}$$

Due to the small dimensions of the satellite and to the nature of the propellant, it is suitable to use a blowdown pressure fed system. This configuration implies the construction of one or two tanks containing a pressurizing gas; in our case, we chose to design two different tanks, one for pressurizing the fuel and one for the oxidizer. This layout is a better choice for safety reasons: in case of damage of one tanks, or failure of one of the lines, the other tank can supply the engine request for both, even tough overall performance is reduced.

The most intuitive configuration, as a first guess, would be a six-cubes satellite, taking into consideration to fit each component in one cube, which are as follows: one for scientific instruments, two gas tanks, one oxidizer tank, one fuel tank and the engine. This premise leads to a first guess on the total mass of the satellite, considering that all the six cubes are filled with the maximum allowed mass, of: $M_0 = 6 \times 1.33\, kg$.

We took this value as the first step of an iterative procedure: at the end of each step, the total mass M_{tot} is computed, accounting for the mass of the propellant, the one of the pressurizing gas and the one of the tanks, all needed to give the required thrust to the guessed mass M_0. Then, the error between M_{tot} and M_0 is computed, as well as a new value for M_0, closer to M_{tot} is selected for the next iteration.

Once imposed the initial guess mass, the necessary mass of propellant is computed from the Tsiolkovky law, considering the required Δv of 600 m/s.

Assessing the current state of the art, we found that, for small-sized satellites, a very high thrust, paired with thrust misalignment and misfire, might lead to irrecoverable destabilization. Furthermore, a lower value of thrust allows a better control. To avoid the aforementioned issues, we chose a thrust value of 3 N [5, p. 3].

2.5 Nozzle and combustion chamber design

First of all, the throat area is found exploiting the chosen value of thrust:

$$A_t = \frac{T}{P_c C_{_T}}$$

Moreover, knowing A_t, and recovering the area ratio set at the beginning, it is possible to compute the exit area of the nozzle.

By using the Rao method, we designed the divergent part of the bell nozzle. Since the dimensions were not exceeding the constraints, we decided to use a full length bell nozzle to minimize the divergent losses. Consulting the graph (see Appendix), we found the final and initial parabola angles, and from those we computed the divergence loss factor

$$\lambda = \frac{1}{2}(1 + \cos(\frac{\alpha + \theta_e}{2}))$$

Then, for the conical convergent part, we considered an inclination angle $\beta = 45deg$ and we computed its initial area as:

$$A_c = \frac{A_t}{M_c}[(\frac{2}{k+1})(1 + \frac{k-1}{k}{M_c}^2)]^{\frac{k+1}{2(k-1)}}$$

having considered a Mach number of $M_c = 0.08$ in the combustion chamber.

The volume of the combustion chamber is computed as: $V_c = L^* A_t$, with a set $L^* = 0.6$. Having the volume and the section area of the combustion chamber, it is possible to

compute its length and then, knowing the angles and the areas of convergent and divergent part, we can obtain the full length of the nozzle.

Both the combustion chamber and the nozzle are designed to be manufactured in rhenium - iridium (Re-Ir) composite material, because of its high resistance over exposure to high temperature conditions for a long time. Its qualities have been proven up to the temperature of 2473 K[9, 10], therefore a regenerative or radiative cooling system might be implemented to keep the temperature of the material at this value. Furthermore, to limit temperature increase, a pulsed firing mode can be chosen: typical frequency values are about 50 Hz [12]. For the later computations, the thrust profile has been considered to be constant so it is possible to obtain the number of firings required to achieve the prescribed Δv.

2.6 Thrust losses

Thrust losses, due to the flow being 2-dimensional and to the boundary layer in the throat area, have been considered. Throat erosion has not been taken into account because of the material used for the nozzle, which experimentally results to be highly resistant to thermal erosion even for long firings [9, 10]. The boundary layer effects are relatively high in small satellites due to the short dimensions of the nozzle, therefore, to take it into account, the discharge coefficient was computed as:

$$C_D = 1 - (\frac{k+1}{2})^{3/4}[3.266 - \frac{2.128}{k+1}]Re^{'-1/2} + 0.9428\frac{(k-1)(k+2)}{(k+1)^{1/2}}Re^{'-1}$$

, where

$$Re^{'} = Re_t\sqrt{\frac{r_t}{0.4\,r_t}}$$

Multiplying C_D and λ, it is possible to obtain the total thrust efficiency, therefore the real thrust of the engine. Hence, the mass flow rate of the propellant, and the burning time afterwards, is obtained.

2.7 Injector design

The challenges we encounter designing a bipropellant engine of this size include the potential of combustion efficiency losses, due to reduced mixing and vaporization which can occur in small engines like this one due to the reduced dimension of the combustion chamber . Additional challenges are related to the accuracy of the injector design. For small flow cross sections, flow rate control, and thus mixture control, can be affected, as a small deviation in the cross sections may lead to large percentage variations in flow rate. In the [3] complex splash- plate or Vortex/Swirl injectors are considered to achieve good combustion and thermal performance.The difficulty in designing and manufacturing these injector elements requires future research and experimental proof. A simpler and acceptable method is to consider a showerhead injector which offers a poor mixing, but is is easier to have it manifold.

The resulting cross section needed by our injectors makes the use of nominal injectors impossible, so we proceeded by designing a specific injector for our needs.

For simplicity of manufacture, a plain atomizer head for the injector was selected. The abrupt change in cross sectional area promotes a turbulent flow, necessary for atomization. The mass flow rate of the oxidizer and fuel injectors can be computed, as the O/F and the propellant mass flow rate are known. Based on the [11] and following Figure 2.5, for the Reynolds numbers obtained and the 0.5 orifice length/diameter ratio, we determined the discharge coefficients Cd for both injectors. A 25% pressure drop across the injection plate was fixed.

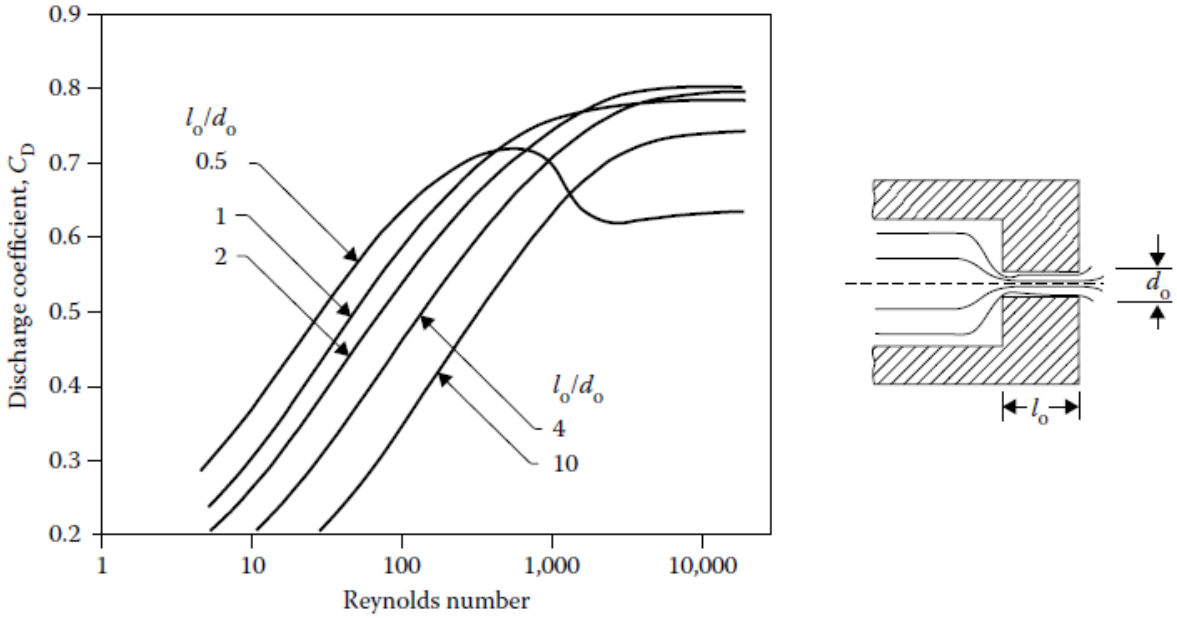

Figure 2.5: Scheme of the injector and discharge coefficient values

At this point, cross sectional area of the injectors and velocities can be computed as follows:

$$A_{inj} = \frac{\dot{m}}{C_d\sqrt{2\Delta P_{inj}\rho}} \qquad v = C_d\sqrt{\frac{2\Delta P_{inj}}{\rho}}$$

2.8 Propellant tanks design

One of the main issues in the design of cubesats is space optimization. For this reason we chose a cylindrical shape for the tanks, which is a good compromise between manufacture simplicity and occupied space.

Moreover, the mass of the fuel and oxidizer carried on board are incremented by 5%, in order to take into account transients, possible leaks, or any other unforeseen issues. In addition to that, the volume of the tanks is considered to be 2% bigger than the propellant volume.

Regarding tanks dimensioning, a radius of 4.5 *cm* was imposed in order to fit in the cubesat accounting for the tank thickness. Thus, the height is computed from the fuel and oxidizer volumes. The pressure of the tank was computed starting from the combustion chamber pressure, adding the pressure drops along the line (injection plates, feed and dynamical ones).

In order to limit the corrosive damage to the inside walls of the tanks, a good solution was to choose stainless steel.The thickness was computed as $t = \frac{P_b\, r}{F_{tu}}$, where F_{tu} is the ultimate tensile strength of steel and P_b is the burst pressure, so the tank pressure multiplied by a safety factor of 1.5.

2.9 Pressurizing gas tank design

When designing the pressurizing gas tanks we have to take into account the freezing temperature of the fuel and oxidizer, since, during the expansion, the gas temperature gets lower. As a first instance, this influences the choice of the gas itself, and in this case we decided to use nitrogen, whose temperature drop with pressure is low. The choice of the initial pressure of the gas has to take into account the pressure needed in the tanks and the final temperature, which can be computed considering an isentropic expansion. The required mass of gas is computed with an iterative cycle, based on the ideal gas law, with an imposed initial pressure of 35 bar (5% of mass has been added as a safety precaution). Moreover, a check is performed so that the final temperature would not be lower than the freezing point of both oxidizer and fuel.

The cylindrical tanks are dimensioned following the same procedure of the propellant tanks, using steel as material and with an imposed radius of 4.5 cm.

2.10 Mass estimation

Regarding the nozzle and the combustion chamber, a thickness of 3 mm has been supposed to compute their mass. For the pipes, instead, we set 15 cm as a reference length, and the thickness has been imposed to 0.5 mm. Two pipes going from the gas tanks to the propellant tanks and two pipes from the propellant tanks to the combustion chamber have been accounted. Considering that the structural mass of each cube is 15% of the maximum possible mass, it is possible to compute the total mass of the satellite M_{tot} as a summation of: scientific instruments, propellant, propellant tanks, gas, gas tanks, structural mass, combustion chamber, nozzle and pipes (the mass of the pipes has been incremented by 5% to take into account the mass of the valves).

Chapter 3

Results calculation

Thanks to the iterative procedure, the total mass of the satellite has highly decreased from the initial guess, thus reducing also the necessary mass of propellant, and therefore the oxidizer and fuel tanks can both fit in one cube. The same happens for the pressurizing gas tanks. This leads to a structure of four cubes: one for the scientific instruments, one for the gas tanks, one for the propellant tanks, and one for the engine, resulting in a total mass of 3.0543 kg.

Table 3.1: Performance parameters evaluation from CEA results (Table 2.2)

P_e $[Pa]$	C^* $[m/s]$	C_T $[-]$	I_s $[s]$	I_{tot} $[N\,s]$	Number of pulses
174.4869	1.6647×10^{-3}	1.7913	303.9737	1660	28062

Table 3.2: Nozzle and combustion chamber sizes (lengths in mm, angles in degrees)

r_t	r_e	r_c	l_c	l_{conv}	l_{div}	l_{tot}	θ_i	θ_e
0.73	8.9	2.0	82.3	1.2	30.6	114.2	32.5	4.5

Table 3.3: Thrust losses, propellant mass and burning time

λ $[-]$	Re $[-]$	C_D $[-]$	T_{real} $[N]$	$\dot{m}_p$ $[kg/s]$	M_p $[kg]$	t_b $[s]$
0.9928	9.4067×10^4	0.9931	2.9577	9.9184×10^{-4}	0.5845	561.25

The resulting thickness in Table 3.5 and 3.6 are taken from the computations explained in the concept description paragraph, where $1.15{\times}10^{-4}$ is the result for the fuel and $1.18{\times}10^{-4}$ is the one for the oxidizer. Since the satellite has to be designed for a long term

Table 3.4: Injectors design

$\dot{m_{ox}}$ $[kg/s]$ $\times 10^{-4}$	$\dot{m_f}$ $[kg/s]$ $\times 10^{-4}$	μ_{ox} $[kg/m\,s]$ $\times 10^{-4}$	μ_f $[kg/m\,s]$ $\times 10^{-4}$	$C_{d,ox}$	$C_{d,f}$	$r_{inj,ox}$ $[mm]$	$r_{inj,f}$ $[mm]$
6.03	3.89	4.10	7.71	0.61	0.62	0.1134	0.1043

Table 3.5: Propellant tanks sizes

	r $[cm]$	h $[cm]$	t $[mm]$	P $[bar]$	m_t $[kg]$	$m_{f/ox}$ $[kg]$
Ox	4.5	4.22	0.5	13.38	0.0966	0.2292
F	4.5	3.93	0.5	13.77	0.0933	0.3553

mission, we decided to increase the thickness up to 0.5 mm in order to take into account corrosion effects and make the manufacturing easier. The same thing has been done for the pressurizing gas tanks and the pipes.

Table 3.6: Pressurizing gas tanks sizes

	r $[cm]$	h $[cm]$	t $[mm]$	P_i $[bar]$	T_f $[K]$	m_t $[kg]$	m_g $[kg]$
Ox	4.5	4.49	0.5	35	226.5	0.0995	0.0108
F	4.5	4.36	0.5	35	228.4	0.098	0.0104

Table 3.7: Final mass estimation (all values in g)

m_{cc}	m_{nozzle}	m_{pipe}	m_f	m_{ox}	$m_{f,t}$	$m_{ox,t}$	$m_{g,f}$	$m_{g,ox}$	$m_{g,f,t}$	$m_{g,ox,t}$	m_{struct}
68.1	64.6	0.074	229.2	355.3	96.6	93.3	10.8	10.4	99.5	98	798

In the end, the total initial mass is 3.0544 kg and the dry mass is 2.4699 kg.

Chapter 4

Concluding remarks

4.1 Failure modes

The complexity of the system requires a good reliability of every component: a malfunction of a simple subsystem can be followed by a chain of failures.

First of all let's consider flaws resulting from manufacturing, especially in the combustion chamber and the nozzle, where pressure is high and one of the hottest temperatures in the whole engine is reached. A defective component can deteriorate quickly, reducing both the operative life and the performance of the whole system.

The small cross section of the injectors and the use of hypergolic propellants could lead to the damage of the injector head, resulting in a different O/F ratio and a modified spraying pattern, thus altering the combustion performance.

Another possible failure can be caused by the leakage of the oxidizer and fuel, whose interaction inside the satellite could lead to the burning of components or even explosion.

Since the engine is conceived for pulsating operation, the combustion products from a previous firing could persist in the combustion chamber and contaminate the next one, thus providing a different thrust output than the one required by the mission.

Considering the architecture of the pressurizing system, should one of the tanks fail, the second tank could support the mission, but its duration would be reduced. This takes into account also a potential failure of the valves.

4.2 Conclusion

The resulting system fulfills the mission requirements by providing the required Δv and respecting all the constraints considered for the project: both the maximum acceleration and the maximum volume and mass for each cube. The use of an iterative procedure allows to optimize the volume and the mass of the satellite, implementing the most compact and lightest possible system considering the constraints. This method even allows to easily expand the system for different missions, by changing the number of cubes and the amount of thrust required. The small dimensions, combined with the complexity of the system, will require a difficult and expensive manufacturing; it is likely that with further research and improvement of production technologies this kind of systems will be easier to make. Even if it is uncommon for the aforementioned complexity reasons, liquid bipropellant engines can be useful in missions that require high thrust, since otherwise it cannot be achieved by more diffused technologies, such as electric propulsion.

Bibliography

[1] Tummala, A.R.; Dutta, A. "An Overview of Cube-Satellite Propulsion Technologies and Trends" *Aerospace* 2017, 4, 58

[2] Páscoa, José; Teixeira, Odelma; Ribeiro, Gustavo "A Review of Propulsion Systems for CubeSats", 10.1115/IMECE2018-88174, July 2018

[3] L. Schoenman, R.L. Friedman, "Low-Thrust bi propellant engine technology", *Final Report*, September 1977 - July 1980

[4] Michael M. Micci, Andrew D. Ketsdever "Micropropulsion for small spacecraft", *Progress in Astronautics and Aeronautics*, Vol. 187, January 2000

[5] Mani, K.; Topputo, F.; Cervone, A. "Chemical Propulsion System Design for a 16U Interplanetary CubeSat" *69th International Astronautical Congress (IAC 2018)*, IAC-18-C4.6.2.x47764, Bremen, Germany, 1-5 Oct. 2018

[6] `https://hyperiontechnologies.nl/`

[7] `https://ntrs.nasa.gov/archive/nasa/casi.ntrs.nasa.gov/20190033329.pdf`

[8] The CubeSat Program, Cal Poly SLO "CubeSat Design Specification", Rev. 13, 20 February 2014

[9] Brian D. Reed, "High-Temperature Oxidation Behavior of Iridium-Rhenium Alloys", *NASA Technical Memorandum 106720*, NASA, 27-29 June 1994, p. 2

[10] Brian D. Reed, James A. Biaglow, Steven J. Schneider "Iridium-Coated Rhenium Radiation-Cooled rockets", *NASA Report*, Lewis Research Center, Cleveland, Ohio, p. 6

[11] Lefebvre, Arthur Henry; McDonell, Vincent G "Atomization and Sprays", 2nd edition, 2017, *Combustion: An International Series*

[12] Xing, Qin; Zhang, Jun; Qian, Menghan; Jia, Zhen-yuan; Sun, Bao-yuan "Thrust stand for low-thrust liquid pulsed rocket engines", September 2010, *The Review of scientific instruments*, Vol. 81

Appendix

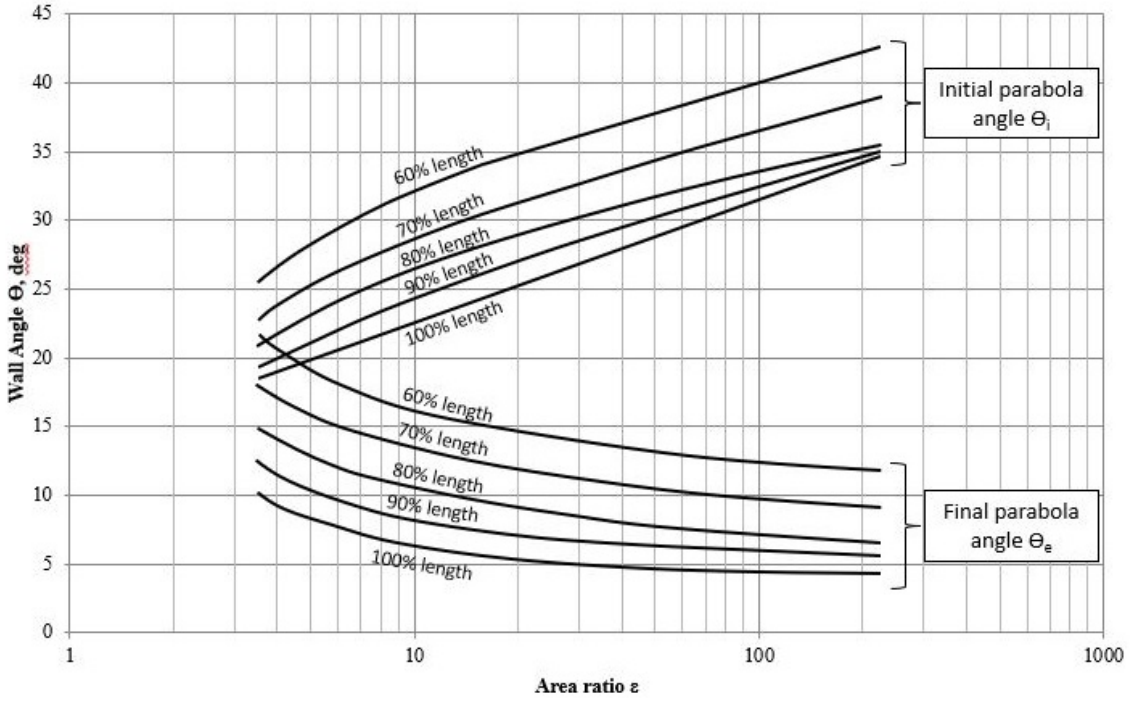

Figure 4.1: Initial and final parabola angles for Rao method